Development of an Innovative Weigh in Motion System for Railway Vehicles

Mirko Ignesti[1], Alice Innocenti[1], Lorenzo Marini[1], Enrico Meli[1], Luca Pugi[1], Andrea Rindi[1]

[1] University of Florence, Department of Industrial Engineering,
via Santa Marta 3. Tel.: +39 0554796479

Abstract

The estimation of the axle loads of running railway vehicles in motion is an important topic in the management of railway networks, basically for purposes of safety and maintenance interventions on the track. To this aim, through a reasonable number of specialized measurement stations, the axle load of the vehicles circulating in a railway network can be easily estimated without any significant consequence on the railway traffic.

In this work the authors present the development of an innovative algorithm for WIM systems aimed at estimating, by means of track measurements, the axle loads of a generic train composition. The formulation of the proposed algorithm is quite general and it can work on different sorts of track measurements (rail shear, rail bending, vertical forces on the sleepers as well as on a combination of them); consequently it can find application in different typologies of measurement stations. The set of experimental physical quantities chosen as inputs are properly treated by the WIM algorithm through estimation procedures based on least square minimization techniques.

This algorithm is shown to be accurate and efficient in a large velocity range and robust as regard the measurement points.

Keywords: *Weigh-in-motion systems, railway track modelling, axle load estimation.*

1 Introduction

The axle load of a railway vehicle is a fundamental parameter which affects both the dynamic behaviour of the vehicle and its impact on the track. The estimation of the axle loads of running vehicles is hence a strategic aspect in the management of railway networks for the sake of running safety, the preservation of the railway track and the planning of maintenance interventions.

The estimation of the axle loads can be conveniently performed by means of specialized measurement stations, without stopping the circulating vehicles and avoiding repercussions on the railway traffic. In that regard, the development of efficient and reliable versions of such measurement systems, usually referred to as *Weigh in Motion systems* (WIM), is interesting from both an industrial and a scientific perspective [1].

The crucial points of a whatever WIM system are surely the performance of the measurement station and above all the characteristics of the algorithm used in the assessment of the unknown loads. In relation to this topic, the following paper deals with an innovative algorithm presented by the authors, through which the estimation of the axle loads can be carried out by exploiting different type of track measurements such as rail shear, rail bending, vertical forces on the sleepers or even by means of whichever their combination. With such prerogatives, the algorithm can find application in different layouts of measurement stations [2]. More precisely, the vertical load of each wheel is deduced from the measurements by assuming that the effects of these unknown loads on the track are approximately superimposable (quasi-linearity hypothesis). With this assumption, the dynamics with which the chosen inputs evolve can be expressed as an opportune weighted combination of the effects provided by a series of single nominal loads moving along the track at the vehicle speed. The set of experimental physical quantities selected as inputs are properly treated by the WIM algorithm through estimation procedures based on least square minimization techniques [3].

As a result, this possibility to use different inputs and measurement layouts guarantees an extrinsic robustness as each physical input is suitable for a certain range frequency; in other words it can be worthwhile to conveniently combine some of them in order to extend the validity of the estimation procedure. Besides this interesting characteristic, the proposed algorithm also features an intrinsic robustness due to the fact that it is based on global techniques, such as least square

minimisation, that work on the overall evolution of the input functions and not only on a few specific parts of them (for instance the peak values).

The testing of the new algorithm has been performed via numerical simulations by using an architecture made up of a detailed 3D multibody model of a two-bogie railway vehicle and an accurate finite element model of the flexible track. In particular the model of the railway line has been developed expressly to test the WIM algorithm with a suitable simulation campaign when experimental data are not available.

To reproduce the real conditions in which the algorithm will be supposed to work, both the physical noise and the measurement noise have also been include in the whole architecture. With regard to the testing campaign, several running conditions of the vehicle have been generated by varying those parameters which have the most influence on the dynamic track response (vehicle speed, car body mass, load distribution etc.). In that regard, such simulation benchmark allowed the robustness of the algorithm performances to be verified considering a broad spectrum of realistic operating conditions.

2 General architecture of the system

The general architecture used for the development of the WIM algorithm is illustrated in Fig. 1 and it consists of two main parts: the physical model and the estimation algorithm. The purpose of this arrangement consists in the optimisation of the algorithm without using any experimental data: the necessary inputs are provided by the physical model by means of numerical simulations of a completely known vehicle passing on the track. Such simulations are performed to obtain dynamic response of the chosen physical inputs which will be used as a benchmark in the estimation process.

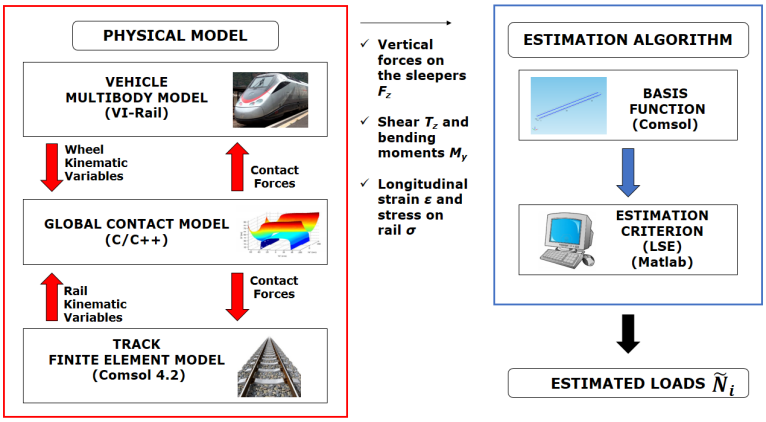

Figure 1. General architecture of the model used in the development of the WIM system.

More precisely, the physical model is formed by two sub-models: the multibody model of the vehicle (implemented with Adams VI-Rail software) and the finite element track model (developed in Comsol environment) that, during the dynamic simulation, interact online through a global contact model developed by the authors in previous works [4, 5]. At each time integration step the multibody model of the vehicle evaluates the kinematic variables (position, orientation and their derivatives) relative to the wheelset and consequently to each wheel. Meanwhile the finite element track model evaluates the kinematic variables (position, orientation and their derivatives) of adequate rail reference systems. The rail and wheel kinematic variables are sent as inputs for the global contact model that calculates the global contact forces and sends these values back both to the vehicle multibody model and to the finite element track model. The data exchange during the simulation (kinematics and contact forces) is performed to reproduce the overall dynamic behaviour of vehicle-track interaction. To this end, the mechanical part of the whole system requires information on the vehicle and on the adopted layout of the measurement station.

The estimation part of the system is made up of the innovative algorithm (implemented in Matlab environment) and of the module for the basis function calculation (developed in Comsol environment). As it will be clarified in detail in chapter 4, the basis functions are a set of elementary solutions concerning the dynamic effect of a single wheel load or axle load on track that leads to the complete reconstruction of the dynamic response of the vehicle on the same track by means of a suitable superimposition. The set of basis function and the way they are superimposed are the core of the estimation procedure. The optimal value of the parameters involved in the algorithm can be found by exploiting the reconstruction of a series of real scenarios, in which the axle or wheels loads of the vehicle are exactly known. As previously introduced, the structure of the estimation algorithm is general and it can manage different kind of physical inputs (strains/forces)

or even a combination of them. During the application, it requires some additional information concerning the vehicle speed, the axle number and the axle positions along the railway vehicle. These further physical quantities can be measured through the utilization of additional sensors or transmitted by the vehicle by means of low cost technologies. In the present research activity the algorithm is based for example on the measurement of the *vertical forces on the sleepers* performed by means of force sensitive elements placed over the sleepers in the section corresponding to the rail baseplate/pads. These forces (simulated F_z if provided by a physical model of the railway track or real F_z^{sp} if coming from experimental data), represent physical inputs of the WIM algorithm that, starting from the knowledge of these physical quantities, estimates the wheel load $\widehat{N}$ through suitable estimation procedures derived from the least squares minimization [6][7][3].

A station for a WIM system consists of some measure points, conveniently distributed along the railway track on the rail foot, depending on the physical quantities to be measured. The number of the measurement points will be as lower as possible to reduce both the station dimensions and the economic costs. On both the sides of the track measure points are present to reject the effect of spurious signals and of load transfers produced by the lateral dynamics.

3 Physical model of the railway track

In order to generate suitable simulation campaigns to test the WIM algorithm when experimental data are not provided, a model involving all components of the track structure and of the vehicle is required. The response of the rail track system is investigated taking into account the vehicle, vehicle speed, contact between wheel and rail, as well as the infrastructure system, considering the interaction between rails, sleeper and ballast.

The physical model consists of a 3D finite element model of the infrastructure (rail, sleepers and ballast), a 3D multibody model of the vehicle and a contact model between the vehicle wheels and the rail. The physical model of the railway track is schematically illustrated in Fig. 2.

The vehicle model and the infrastructure model interact online during the simulations by means of a 3D global contact model, specifically developed to improve reliability and accuracy of the contact points detection [4, 5]. In the rest of the paper x_{ai} denotes the initial position of the $i-th$ axle of the vehicle (the total number of the axles is n_{tot}), F_{zs}^k is the vertical force on the sleeper relating the $k-th$ measure point x_{mk}^s of the measure station ($s = left, right$), while the generic vertical wheel load is N_{is} where $s = left, right$ and V is the velocity. The corresponding estimated load $\widehat{N}_{is}$ will be computed by the presented WIM algorithm; the weights of the wheels are included in the loads $\widehat{N}_{is}$, N_{is}. Anyway the proposed approach can be easily used both for wheel and axle loads measurements. In fact, in case of axle load estimation, a similar procedure can be applied by considering $\widehat{N}_i$, N_i as the vertical loads on the single axle.

3.1 The infrastructure model

Rail and underlaying infrastructures are modeled as 3D beams, which take into account all the six degrees of the rail (displacements u_{rail}, v_{rail}, w_{rail} and rotations ϑ_{xrail}, ϑ_{yrail}, ϑ_{zrail}), supported by an elastic discrete foundation representing sleepers and ballast. Therefore, the track deflection is described by means of a model which comprises 3D beams connected through visco-elastic elements to n_{sl} 2D rigid bodies representing rail sleepers, which are in turn supported by a visco-elastic foundation including the ballast properties.

According to literature [1], for the rail modeling, both Eulero-Bernoulli and Rayleigh-Timoshenko theories can be used. In the present work the Rayleigh-Timoshenko beam model has been adopted; this theory includes rotatory inertia and shear deformation of the beam (see Fig. 3). Hence, for example, the beam vertical displacement is ruled through the partial differential equation:

$$EI\frac{\partial^4 w(x,t)}{\partial x^4} + \rho A\frac{\partial^2 w(x,t)}{\partial t^2} - \rho I\left(1+\frac{E}{kG}\right)\frac{\partial^4 w(x,t)}{\partial x^2 \partial t^2} + \frac{\rho^2 I}{kG}\frac{\partial^4 w(x,t)}{\partial t^4} = q(x,t) + \frac{\rho I}{kGA}\frac{\partial^2 q}{\partial t^2} - \frac{EI}{kGA}\frac{\partial^2 q}{\partial x^2} \qquad (1)$$

where $x \in [L_I, L_F]$ is the longitudinal abscissa, $t \in [T_I, T_F]$ is the time, E and ρ are the Young modulus and the density of the beam, A and I are the area and the momentum of the beam section, G is the shear modulus, k is the shear factor and $q(x,t)$ is the distributed load and $w(x,t)$ is the vertical displacement. The initial conditions associated to Eq. 1 are $w(x,T_I) = 0 \ \ \forall x \in [L_I, L_F]$ and $\frac{\partial w}{\partial t}(x,T_I) = 0 \ \ \forall x \in [L_I, L_F]$ respectively, while there are no boundary conditions because the beam is connected only to the sleepers as will be better clarified in the following chapters.

In this work the UIC60 rail profile canted at $1/20$ rad has been adopted. The main physical characteristics of the rail beam model are listed in Tab. 1. The length of the track studied in the model is 72 m. The separation distance between two contiguos sleepers is equal to 0.60 m.

The sleepers are modeled as 2D rigid bodies connected to the rails by means of visco-elastic elements including lateral k_{ysl}, vertical k_{zsl} and rotational $k_{\vartheta sl}$ stiffness and lateral c_{ysl}, vertical c_{zsl} and rotational $c_{\vartheta sl}$ damping properties.

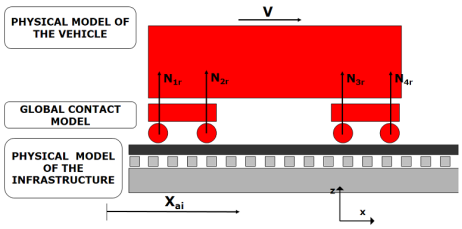

Figure 2. The physical model of the railway track.

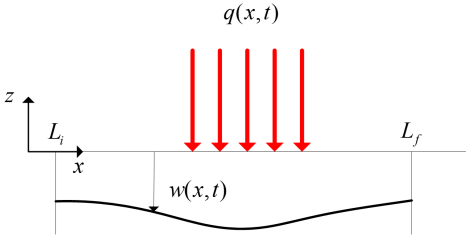

Figure 3. Beam model of the rail.

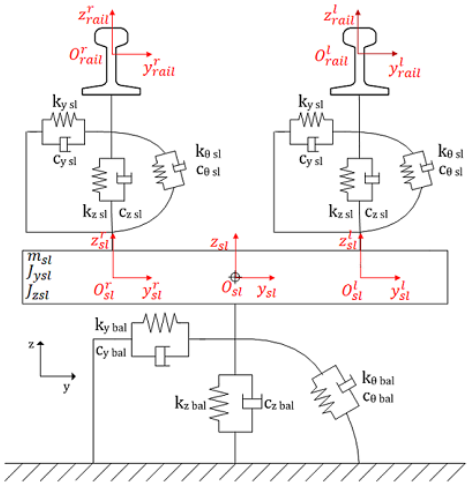

Figure 4. Rail and sleepers reference systems.

The generic 2D sleeper is supported by a flexible foundation characterizing the behaviour of the ballast through the lateral k_{ybal}, vertical k_{zbal} and rotational $k_{\vartheta bal}$ stiffness values and lateral c_{ybal}, vertical c_{zbal} and rotational $c_{\vartheta bal}$ damping values. The 3DOF system modeling the sleeper-ballast ensemble is described by the lateral v_{sl} and vertical w_{sl} translations and the rotation ϑ_{sl} around the $x_{sl}-axis$ of the sleeper reference system.

Table 1. Main characteristics of the rail beam model

Parameter	Units	Value
Young modulus E	Pa	$2.1*10^{11}$
Density ρ	kg/m^3	$7.8*10^3$
Area of the beam section A	m^2	$7.686*10^{-3}$
Momentum of the beam section I	m^4	$3.055*10^{-5}$
Rayleigh damping coefficient α_r	s^{-1}	30
Rayleigh damping coefficient β_r	s	0.003
Distance between neutral section and rail foot z_f	m	-0.172
Shear factor k		0.4

Hence, the dynamic model of the sleeper can be expressed through the following equation:

$$\mathrm{M}\ddot{\mathbf{v}}_{sl}+\mathrm{K}_{sl\,l}(\mathbf{v}_{sl\,l}-\mathbf{v}_{rail\,l})+\mathrm{C}_{sl\,l}(\dot{\mathbf{v}}_{sl\,l}-\dot{\mathbf{v}}_{rail\,l})+\mathrm{K}_{sl\,r}(\mathbf{v}_{sl\,r}-\mathbf{v}_{rail\,r})+\mathrm{C}_{sl\,r}(\dot{\mathbf{v}}_{sl\,r}-\dot{\mathbf{v}}_{rail\,r})+\mathrm{K}_{bal}\mathbf{v}_{sl}+\mathrm{C}_{bal}\dot{\mathbf{v}}_{sl}=0 \quad (2)$$

where subscript sl refers to the sleeper, subscript bal indicates the ballast properties, subscript $rail$ refers to the rail and l,r the rail side. Vector $\mathbf{v}_{sl}$ includes lateral v_{sl}, vertical w_{sl} and rotational ϑ_{sl} displacements of the sleeper reference system $O_{sl}x_{sl}y_{sl}z_{sl}$ placed in the sleeper center of mass (see Fig. 4); M is the sleeper mass matrix while K_{bal} and C_{bal} are respectively the stiffness and damping matrix of the ballast. Using index s to indicate the rail side ($s=left,right$), the vectors $\mathbf{v}_{sl\,s}$ define lateral $v_{sl\,s}$, vertical $w_{sl\,s}$ and rotational $\vartheta_{sl\,s}$ displacement respectively of the left and right sleeper reference systems $O^s_{sl}x^s_{sl}y^s_{sl}z^s_{sl}$, while $\mathbf{v}_{rail\,s}$ define lateral $v_{rail\,s}$, vertical $w_{rail\,s}$ and rotational $\vartheta_{rail\,s}$ displacement of left and right beam respectively in the left and right rail reference systems $O^s_{rail}x^s_{rail}y^s_{rail}z^s_{rail}$. K_{sl} and C_{sl} are respectively the stiffness and damping matrix characterizing the rail/sleeper visco-elastic connection.

The rail/sleeper interaction forces (F_{ys}, F_{zs} and M_{xs}) can be easily obtained starting from the eq. 2 and they are modeled by means of $2n_{sl}$ point loads acting on the 3D beams, applied in correspondence of the discrete support locations, representing the rail/sleeper interface.

The numerical results have been obtained using the IDA solver [8, 9], which uses variable-order variable step-size backward differentiation formulas (BDF) for the time integration; the algorithm MUMPS has been employed to solve the linear systems arising from the FE discretisation of the rail beams. Tab. 2 sums up the values of the main parameters of the ODE integrator like the maximum step size *MaxStep*, the absolute and relative tolerance *AbsTol RelTol* and the maximum dimension h_{max} of the element of the rails mesh.

Table 2. Parameters of the ODE integrator.

Parameters	Unit	Value
MaxStep	s	10^{-4}
AbsTol	–	10^{-5}
RelTol	–	10^{-6}
h_{max}	m	0.001

Table 3. Inertia properties of the multibody model.

MBS body	Mass kg	Roll Inertia kgm^2	Pitch Inertia kgm^2	Yaw Inertia kgm^2
Car body	32000	56800	1970000	1970000
Bogie	2615	1722	1476	3067
Wheelset	2091	1120	112	1120

3.2 The vehicle model

The railway vehicle chosen for the dynamic simulations is the Manchester Wagon, the mechanical structure and elastic and damping characteristics of which are easily available in the literature [10]; in Tab. 3 the inertia properties of the vehicle are shown. The multibody 3D model of this vehicle has been studied and validated in different conditions. Consequently, the model can be considered a reliable benchmark for the evaluation of the performances of the proposed WIM algorithm. The multibody 3D model of the Manchester Wagon, implemented in the Adams VI-Rail environment, is schematically shown in Fig. 5. The vehicle is formed by the car body (Fig. 5), two bogies (Fig. 6) and four wheelsets (Fig. 7).

The rigid bodies are connected by means of appropriate elastic and damping elements; particularly the vehicle is equipped with two suspension stages. Both the suspension stages have been modeled by three-dimensional nonlinear force elements like bushings, dampers, and bumpstops (see Figs. 6 and 7).

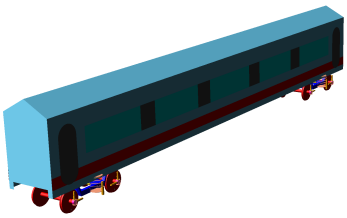

Figure 5. Global view of the multibody model.

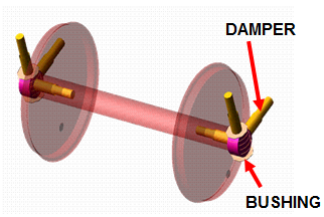

Figure 6. Primary suspensions.

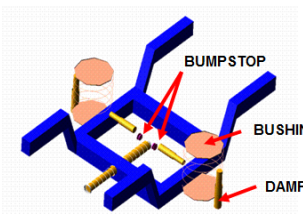

Figure 7. Secondary suspensions.

The vehicle and the infrastructure models interact online during the simulations through a 3D global contact model, specifically developed to improve reliability and accuracy of the contact points detection. In particular the adopted contact model [4, 5] is based on a two step procedure; the contact points detection and the global contact forces evaluation.

3.3 Measurement error

To improve the accuracy of the physical model of the railway track, the following disturbances have been considered:

- *frequency effects on the signal F_{zs}^k due to the limited band of physical system and measurement chain*: the frequency effects due to the limited band of the real system and the rail measurement chain have been modelled through a second order low pass filter directly applied to the physical signals F_{zs}^k relative to the measure points x_{mk}^s of the measurement station:

$$F_{zs}^{fk}(t) = B_{2,\omega_n}(s) F_{zs}^k(t) \tag{3}$$

  where $B_{2,\omega_n}(s)$ is the second order Butterworth filter and $\omega_n = 2\pi f_n$ is the cut frequency (ω_n in rad/s and f_n in Hz).

- *numerical disturbances and bias errors on the signal F_{zs}^{fk}*: besides the frequency effects, also numerical disturbances and bias errors on the signal F_{zs}^{fk} have been modelled:

$$F_{zs}^{fr^k}(t) = F_{zs}^{fk}(t) + U_F^k[\mu_F, \delta_F/2] \tag{4}$$

  where μ_F and δ_F are the mean and the amplitude of the disturbance distribution U_F^k. The aim of numerical disturbances and bias errors on the signal F_{zs}^{fk} consists in properly reproducing the numerical noise affecting the measurement; therefore they have to be applied to the signal only after the low pass filter.

The measurement errors will play a fundamental role when the physical model of the railway track will be employed to test the accuracy and the stability of the WIM algorithm in absence of experimental data.

4 WIM algorithm

In this chapter the innovative WIM algorithm for the estimation of the vertical wheel loads $\widehat{N}$ on railway vehicles is described (the weights of the wheels are included in the loads $\widehat{N}$). As previously stated, the WIM system is based on the measurements of vertical forces on the sleepers F_z performed by means of force sensitive element placed over the sleepers in the section corresponding to the rail baseplate/pads.

4.1 Architecture of the WIM algorithm

The general architecture of the system is described in the diagram in Fig. 8. The developed WIM algorithm performs the estimation $\widehat{N}_{is}$ of the vertical wheel loads N_{is} starting from the knowledge of the simulated $F_{zs}^{fr\,k}$ or experimental $F_{zs}^{sp\,k}$ vertical forces relative to the measure points x_{mk}^{s} of the measurement station; in absence of numerical disturbances the vertical forces on the sleepers F_{zs}^{fr} will be equal to the original signal F_{zs}. Moreover the WIM algorithm also needs some additional information (external inputs) concerning the vehicle speed V, the axle number n_{tot} and the axle positions inside the railway vehicle x_{ai}. These further physical quantities can be identified using by example additional sensors or transmitted by the vehicle itself using low cost technologies. Obviously the WIM algorithm can work both with synthetic inputs provided by numerical models and with experimental data directly measured on the railway track; in this second case the algorihm inputs (F_{zs}^{sp}, V^{sp}, n^{sp}, and x_a^{sp}) will be marked with the apex sp.

The main idea behind the new WIM algorithm arises from the observation that the wheels layout turns out to be a good approximation of the whole railway track model. At this point, because of the simple structure of the wheels layout, it is quite intuitive to suppose the system approximatively linear with respect to the vertical loads N_{is} (the so-called *quasi-linearity hypothesis* (QLH)); in other words the effect of the generic load N_{is} on the vertical forces on the sleeper $F_{zs}^{fr\,k}$ or $F_{zs}^{sp\,k}$ is assumed not to be affected by the presence of the other loads (especially the contiguous ones). Therefore, by applying the superposition principle, it is possible to estimate both the simulated vertical forces on the sleepers $F_{zs}^{fr\,k}$ and the experimental ones $F_{zs}^{sp\,k}$ produced by the whole train through a linear combination of n_{tot} forces $\mathfrak{B}_{zs}^{ki}$ produced by n_{tot} single fictitious loads N_{fs} (one for each vehicle wheel) properly shifted in the time of a delay t_i. Evidently, in order to correctly apply the superposition of effects, the *quasi-linearity hypothesis* (QLH) must hold within the whole range of velocities V and cut frequencies f_n considered for railway vehicles.

The fictitious load N_{fs} represents the load on the wheels and also includes the weight of the wheel. In this case the linear combination coefficients are equal to $\widehat{N}_{is}/N_{fs}$. Obviously, since the system can be considered only approximatively linear, a *least squares optimization* (LQO) is needed to minimize the approximation error and, at the same time, to optimize the values of $\widehat{N}_{is}$.

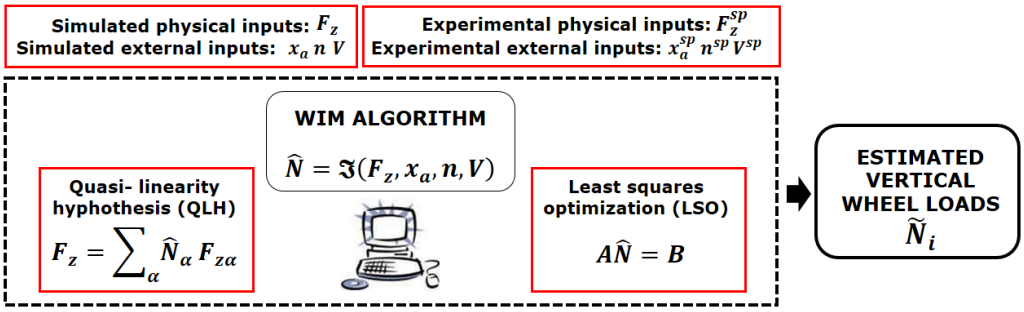

Figure 8. Architecture of the WIM algorithm

4.2 The quasi-linearity hypothesis

At this preliminary phase of the research activity, the model of the track used in the fictitious system (to evaluate the basis functions) is analogous to the one used to simulate the physical model of the railway track, previously described in chapter 3.1. This model may be simplified in order to evaluate the robustness of the WIM algorithm as regard real track data.

The position of the fictitious load N_{fs} along the track, the relative vertical force on the sleeper $\mathfrak{B}_{zs}^{k}$, the simulated and experimental force on the sleeper F_{zs}^{frk}, F_{zs}^{spk} are defined as:

$$\mathfrak{B}_{zs}^{k}(t) = \mathfrak{B}_{zs}(x_{mk}^{s}, t) \qquad x_f = x_{af} + t * V \tag{5}$$

$$F_{zs}^{frk}(t) = F_{zs}^{frk}(x_{mk}^{s}, t) \tag{6}$$

$$F_{zs}^{spk}(t) = F_{zs}^{spk}(x_{mk}^{s}, t) \tag{7}$$

where $x_{af} = 0$ m and $t \in [T_I, T_F]$. In this way the n_{tot} vertical forces on the sleepers $\mathfrak{B}_{zs}^{ki}$ produced by n_{tot} single fictitious loads N_{fs} and their positions x_{fi} can be evaluated by introducing suitable time delays $t_i = \frac{x_{ai} - x_{af}}{V}$ and by applying such delays to the vertical forces on the sleepers $\mathfrak{B}_{zs}^{k}$ and the position x_f:

$$\mathfrak{B}_{zs}^{ki}(t) = \mathfrak{B}_{zs}^{k}(t + t_i) \qquad x_{fi} = x_{af} + (t + t_i) * V = x_{ai} + t * V = x_i \tag{8}$$

where $t \in [T_I, T_F - t_i]$. At this point, thanks to the superposition principle, both the simulated vertical forces on the sleepers $F_{zs}^{fr\,k}$ and the experimental ones $F_{zs}^{sp\,k}$ produced by the whole train can be approximated as follows:

$$F_{zs}^{fr\,k}(t) \simeq F_{zs\,ap}^{fr\,k}(t) = \sum_{i=1}^{n_{tot}} \alpha_{is}^{sim} \mathfrak{B}_{zs}^{ki}(t) \qquad \alpha_{is}^{sim} = \frac{\hat{N}_{is}^{sim}}{N_{fs}} \qquad k = 1, 2, ...N_m \qquad s = left, rail \tag{9}$$

$$F_{zs}^{sp\,k}(t) \simeq F_{zs\,ap}^{sp\,k}(t) = \sum_{i=1}^{n_tot} \alpha_{is}^{sp} \mathfrak{B}_{zs}^{ki}(t) \qquad \alpha_{is}^{sp} = \frac{\hat{N}_{is}^{sp}}{N_{fs}} \qquad k = 1, 2, ...N_m \qquad s = left, rail \tag{10}$$

where, as said before, the linear combination coefficients α_{is}^{sim}, α_{is}^{sp} are proportional to the estimated vertical loads $\widehat{N}_{is}^{sim}$ and $\widehat{N}_{is}^{sp}$.

4.3 Least squares estimation

Since the studied problem is only approximatively linear, a *least squares optimization* (LQO) is needed to minimize the approximation error between $F_{zs}^{fr\,k}$, $F_{zs}^{sp\,k}$ and $F_{zs\,ap}^{fr\,k}$, $F_{zs\,ap}^{sp\,k}$ and, at the same time, to optimize the values of $\widehat{N}_{is}^{sim}$, $\widehat{N}_{is}^{sp}$. In this specific case linear not-weighted least squares have been considered [7]. To simulate the sampling due to the measurement process, the time domain $t \in [T_I, \bar{T}_F], \bar{T}_F = T_F - t_1$ (the shortest one among the domains $t \in [T_I, \hat{T}_F], \hat{T}_F = T_F - t_i$) has been discretized with the a sample time equal to $\Delta t = 0.001s$. Therefore both the simulated vertical forces on the sleepers $F_{zs}^{fr\,k}(t_h)$ and the experimental ones $F_{zs}^{sp\,k}(t_h)$ are known only at the times t_h with $h = 1, 2, ...N_s$ (N_s is the samples number while $t_1 = T_I$ and $t_{N_s} = \bar{T}_F$); the same time discretization holds also for the fictitious vertical forces $\mathfrak{B}_{zs}^{ki}(t_h)$ employed to estimate $F_{zs}^{fr\,k}$, $F_{zs}^{sp\,k}$ (see Eq. 9 and 10). The sampled quantities can be written as

$$\mathbf{F}_{zs}^{fr\,k} = \begin{bmatrix} F_{zs}^{fr\,k}(t_1) \\ \vdots \\ F_{zs}^{fr\,k}(t_h) \\ \vdots \\ F_{zs}^{fr\,k}(t_{N_s}) \end{bmatrix} \in R^{N_s} \quad \mathbf{F}_{zs}^{sp\,k} = \begin{bmatrix} F_{zs}^{sp\,k}(t_1) \\ \vdots \\ F_{zs}^{sp\,k}(t_h) \\ \vdots \\ F_{zs}^{sp\,k}(t_{N_s}) \end{bmatrix} \in R^{N_s} \quad \mathfrak{B}_{zs}^{ki} = \begin{bmatrix} \mathfrak{B}_{zs}^{ki}(t_1) \\ \vdots \\ \mathfrak{B}_{zs}^{ki}(t_h) \\ \vdots \\ \mathfrak{B}_{zs}^{ki}(t_{N_s}) \end{bmatrix} \in R^{N_s}. \tag{11}$$

Taking into account the time sampling, Eq. 9 and 10 become

$$F_{zs}^{fr\,k}(t_h) \simeq \sum_{i=1}^{n_{tot}} \alpha_{is}^{sim} \mathfrak{B}_{zs}^{ki}(t_h) \qquad h = 1, 2, ...N_s \qquad k = 1, 2, ...N_m \qquad s = left, rail \tag{12}$$

$$F_{zs}^{sp\,k}(t_h) \simeq \sum_{i=1}^{n_{tot}} \alpha_{is}^{sp} \mathfrak{B}_{zs}^{ki}(t_h) \qquad h = 1, 2, ...N_s \qquad k = 1, 2, ...N_m \qquad s = left, rail \tag{13}$$

At this point, defining the matrix $A_s \in R^{N_s N_m \times n_{tot}}$ and the vectors $\mathbf{b}_s^{fr} \in R^{N_s N_m}$, $\mathbf{b}_s^{sp} \in R^{N_s N_m}$ as follows:

$$A_s = \begin{bmatrix} \mathfrak{B}_{zs}^{11} & \dots & \mathfrak{B}_{zs}^{1n_1} & \dots & \mathfrak{B}_{zs}^{1n_{tot}} \\ & & \vdots & & \\ \mathfrak{B}_{zs}^{k1} & \dots & \mathfrak{B}_{zs}^{kn_1} & \dots & \mathfrak{B}_{zs}^{kn_{tot}} \\ & & \vdots & & \\ \mathfrak{B}_{zs}^{N_m 1} & \dots & \mathfrak{B}_{zs}^{N_m n_1} & \dots & \mathfrak{B}_{zs}^{N_m n_{tot}} \end{bmatrix} \qquad \mathbf{b}_s^{fr} = \begin{bmatrix} \mathbf{F}_{zs}^{fr\,1} \\ \vdots \\ \mathbf{F}_{zs}^{fr\,k} \\ \vdots \\ \mathbf{F}_{zs}^{fr\,N_m} \end{bmatrix} \quad \mathbf{b}_s^{sp} = \begin{bmatrix} \mathbf{F}_{zs}^{sp\,1} \\ \vdots \\ \mathbf{F}_{zs}^{sp\,k} \\ \vdots \\ \mathbf{F}_{zs}^{sp\,N_m} \end{bmatrix}, \tag{14}$$

the matrix form of Eq. 12 and 13 can be obtained:

$$\mathbf{b}_s^{fr} \simeq A_s \boldsymbol{\alpha}_s^{sim} \qquad \mathbf{b}_s^{sp} \simeq A_s \boldsymbol{\alpha}_s^{sp} \tag{15}$$

where:

$$\boldsymbol{\alpha}_s^{sim} = \begin{bmatrix} \alpha_{1s}^{sim} & \dots & \alpha_{n_1 s}^{sim} & \dots & \alpha_{n_{tot} s}^{sim} \end{bmatrix}^T \in R^{n_{tot}} \qquad \boldsymbol{\alpha}_s^{sp} = \begin{bmatrix} \alpha_{1s}^{sp} & \dots & \alpha_{n_1 s}^{sp} & \dots & \alpha_{n_{tot} s}^{sp} \end{bmatrix}^T \in R^{n_{tot}}. \tag{16}$$

By means of a *least squares optimization* (LQO) (in this case linear and not-weighted), it is now possible to minimize the squared 2-norms $E_s^{fr2} = \left\|\mathbf{E}_s^{fr}\right\|_2^2$ and $E_s^{sp2} = \left\|\mathbf{E}_s^{sp}\right\|_2^2$ of the approximation errors $\mathbf{E}_s^{fr} = A_s\boldsymbol{\alpha}_s^{sim} - \mathbf{b}_s^{fr}$, $\mathbf{E}^{sp} = A_s\boldsymbol{\alpha}_s^{sp} - \mathbf{b}_s^{sp}$ present in Eq. 15:

$$\boldsymbol{\alpha}_s^{sim} = \left(A_s^T A_s\right)^{-1} A_s^T \mathbf{b}_s^{fr} \qquad\qquad \boldsymbol{\alpha}_s^{sp} = \left(A_s^T A_s\right)^{-1} A_s^T \mathbf{b}_s^{sp} \tag{17}$$

where the matrix $A_s^T A_s$ is invertible only if the rank of A_s is maximum. Finally the values of the estimated vertical loads $\widehat{N}_{is}^{sim}$, $\widehat{N}_{is}^{sp}$ can be evaluted starting from the knowledge of $\boldsymbol{\alpha}_s^{sim}$ and $\boldsymbol{\alpha}_s^{sp}$:

$$\widehat{\mathbf{N}}_s^{sim} = N_{fs}\boldsymbol{\alpha}_s^{sim} \qquad\qquad \widehat{\mathbf{N}}_s^{sp} = N_{fs}\boldsymbol{\alpha}_s^{sp} \tag{18}$$

where:

$$\widehat{\mathbf{N}}_s^{sim} = \left[\begin{array}{ccccccc} \widehat{N}_{1s}^{sim} & \dots & \widehat{N}_{n_1 s}^{sim} & \dots & \widehat{N}_{n_{tots}}^{sim} \end{array}\right]^T \in R^{n_{tot}} \qquad\qquad \widehat{\mathbf{N}}_s^{sp} = \left[\begin{array}{ccccccc} \widehat{N}_{1s}^{sp} & \dots & \widehat{N}_{n_1 s}^{sp} & \dots & \widehat{N}_{n_{tot}s}^{sp} \end{array}\right]^T \in R^{n_{tot}} \tag{19}$$

5 Performance of the WIM algorithm

This chapter describes the performance of the WIM algorithm for the estimation of the vertical wheel loads $\widehat{N}_s$ starting from the knowledge of the vertical loads on the sleepers F_{zs}.

The WIM algorithm has been tested with a suitable simulations campaign to verify the accuracy of the procedure when experimental data are not available; to this aim the whole physical model of the railway track has been developed (see chapter 3). The attention is focused on the influence of vehicle velocity V and cut frequency f_n of the physical system. In this second phase the measurement errors play a foundamental role to evaluate the robustness of the WIM algorithm in any operating condition.

In this chapter the vertical forces on the sleepers $F_{zs}^{fr\,k}(t) = F_{zs}^{fr}(x_{mk}^s, t)$ evaluated through the physical model of the railway track (see chapter 3) are compared with the vertical forces on the sleepers $F_{zs\;ap}^{fr\,k}(t) = F_{zs\;ap}^{fr}(x_{mk}^s, t)$ estimated by means of the WIM algorithm (see Eq. 9 and see Fig. 9). The comparison between the vertical forces calculated by the physical model and those estimated by the WIM procedure is quite important to test the algorithm accuracy when experimental data are not available. Furthermore in this case the measurement errors will be considered (according to chapter 3.3) in order to evaluate the algorithm robustness in presence of disturbances.

The considered measure station is characterized by a layout with a number $N_m = 2$ of measure points on both rail side and a distance $l_k = 5.4$ m between the two consecutive measure points ($x_{m1}^s = 32.4$ m and $x_{m2}^s = 37.8$ m).

In this work the dependence of the relative errors $e_{is}^{sim} = \frac{\widehat{N}_{is}^{sim} - N_{is}}{N_{is}}$ on the vehicle speed V and the cut frequency f_n of the physical system is analysed. In Tab. 4 the considered variation ranges for the previous quantities are reported.

Table 4. Variation ranges of V and f_n adopted for the simulations campaign and their discretization

Velocity	Unit	Value	Cut frequency	Units	Value
Min. train velocity V_{min}	$\mathrm{m\,s^{-1}}$	10	Min cut off freq. f_{nmin}	Hz	20
Max. train velocity V_{max}	$\mathrm{m\,s^{-1}}$	100	Max cut off freq. f_{nmax}	Hz	40
Sim. number N_v	–	10	Sim. number N_{fn}	–	2
$\Delta V = (V_{max} - V_{min})/(N_v - 1)$	$\mathrm{m\,s^{-1}}$	10	$\Delta f_n = (f_{nmax} - f_{nmin})/(N_{fn} - 1)$	Hz	20
$V_I = V_{min} + (I-1)\Delta V$, $I = 1,...N_v$			$f_{nJ} = f_{nmin} + (J-1)\Delta f_n$, $J = 1,...N_{fn}$		

By way of example Fig. 9 shows the vertical force on sleepers adding numerical disturbances taken from both the measure points on right rail side (the original $F_{zs}^{fr\,k}$ and the approximated $F_{zs\;app}^{fr\,k}$) relative to the simulation performed at a speed of $V = 40\ \mathrm{m\,s^{-1}}$. As can be seen in the figure, the differences between the plotted quantities are quite negligible.

The global performance of the WIM algorithm have been studied by considering the maximum relative error $e_{\max}^{sim}(V, f_n)$

$$e_{\max}^{sim} = \left\|\mathbf{e}^{sim}\right\|_\infty = \max_{1 \le i \le n_j,\ s=l,r} \left|e_{is}^{sim}\right| \qquad\qquad \mathbf{e}_{is}^{sim} = \left[\begin{array}{ccccc} e_{1s}^{sim} & \dots & e_{n_1 s}^{sim} \end{array}\right]^T \in R^{n_{tot}} \tag{20}$$

and analysing the maximum error values $e_{\max}^{sim}(V, f_n)$.

The values of the nominal N_{is}^{sim} and estimated $\widehat{N}_{is}^{sim}$ loads on the vehicle wheels evaluated in a test performed with a vehicle speed $V = 50\ \mathrm{m\,s^{-1}}$ are listed in Tab. 5. Tab. 5 also summarizes the relative errors e_{is}^{sim}. The algorithm accuracy in estimating the vertical loads (relative errors equal to $0.2 - 1.8\%$) is mainly due to the capability in correctly describing

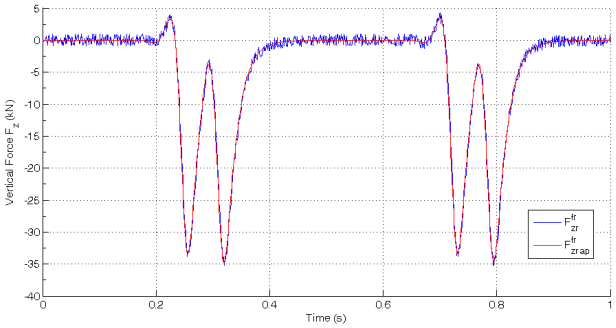

(a) First measure point on right rail side x^r_{m1}

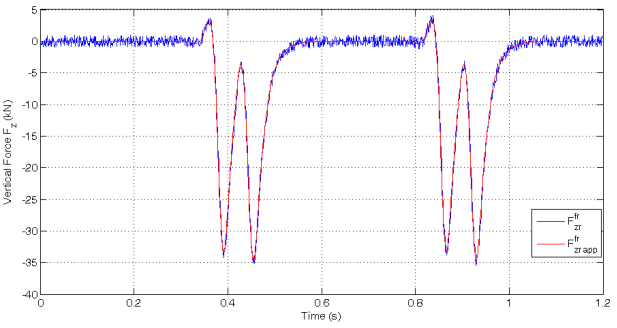

(b) Second measure point on right rail side x^r_{m2}

Figure 9. Comparison between the vertical load obtained with the wheels layout of the vehicle model $F_{zs}^{fr\ k}(t)$ and with fictitious vertical loads $F_{zs\ app}^{f\ k}(t)$ according to the *quasi-linearity hypothesis.*

the global shape of the solutions (both in space and in time). Tab. 5 shows a quite large accuracy of the WIM algorithm even for relatively low values of f_n.

Tab. 6 lists the nominal N_{is}^{sim} and estimated loads on the vehicle wheels $\widehat{N}_{is}^{sim}$ for test performed with a vehicle speed $V = 100$ m s^{-1}. In this case, despite of the very high value of V, the maximum relative error value (7.1% with $f_n = 20$ Hz) is less than 10%. The maximum relative error values $e_{\max}^{sim}(V, f_n)$ are plotted as a function of both velocity V and cut frequency f_n.

Table 5. Estimated vertical loads on the vehicle wheels, $\widehat{N}_{is}^{sim}$: vehicle velocity $V = 50m/s$.

Cut frequency f_n Hz	Parameter	Value N	Parameter	Value %
20	$\widehat{N}_{1r}^{sim}$	51264	e_{1r}^{sim}	1.6%
40		51714		0.7%
20	$\widehat{N}_{1l}^{sim}$	51137	e_{1l}^{sim}	1.8%
40		51587		1.0%
20	$\widehat{N}_{2r}^{sim}$	51829	e_{2r}^{sim}	0.5%
40		51900		0.3%
20	$\widehat{N}_{2l}^{sim}$	51887	e_{2l}^{sim}	0.3%
40		51958		0.2%
20	$\widehat{N}_{3r}^{sim}$	51166	e_{3r}^{sim}	1.8%
40		51611		0.9%
20	$\widehat{N}_{3l}^{sim}$	51152	e_{3l}^{sim}	1.8%
40		51596		0.9%
20	$\widehat{N}_{4r}^{sim}$	51748	e_{4r}^{sim}	0.6%
40		51815		0.5%
20	$\widehat{N}_{4l}^{sim}$	51497	e_{4l}^{sim}	1.1%
40		51565		1.0%

Table 6. Estimated vertical loads on the vehicle wheels, $\widehat{N}_{is}^{sim}$: vehicle velocity $V = 100m/s$.

Cut frequency f_n Hz	Parameter	Value N	Parameter	Value %
20	$\widehat{N}_{1r}^{sim}$	48380	e_{1r}^{sim}	7.1%
40		50504		3.0%
20	$\widehat{N}_{1l}^{sim}$	48875	e_{1l}^{sim}	6.2%
40		51003		2.1%
20	$\widehat{N}_{2r}^{sim}$	52585	e_{2r}^{sim}	1.0%
40		52639		1.1%
20	$\widehat{N}_{2l}^{sim}$	52687	e_{2l}^{sim}	1.2%
40		52741		1.2%
20	$\widehat{N}_{3r}^{sim}$	48573	e_{3r}^{sim}	6.7%
40		50700		2.7%
20	$\widehat{N}_{3l}^{sim}$	47972	e_{3l}^{sim}	7.9%
40		50095		3.8%
20	$\widehat{N}_{4r}^{sim}$	52346	e_{4r}^{sim}	0.5%
40		52399		0.6%
20	$\widehat{N}_{4l}^{sim}$	52475	e_{4l}^{sim}	0.8%
40		52529		0.9%

6 Conclusions and further developments

In this paper the authors presented an innovative WIM algorithm with the aim of estimating the vertical wheel loads $\widehat{N}_{is}$ of railway vehicles. In this particular case the algorithm is based on *vertical forces on the sleepers* F_z performed through force sensitive elements placed over the sleepers in the section corresponding to the rail baseplate/pads. These physical quantities are then properly organized and processed by means of suitable estimation procedures derived from the least squares minimization that allow the calculation the wheel loads $\widehat{N}_{is}$. The WIM system employes various measure points placed along the railway track on the sleepers.

The authors have also developed a physical model of the railway track to test the WIM algorithm with a suitable simulation campaign when experimental data are not available. The results of the new WIM algorithm highlighted a good agreement between the estimated quantities and the simulated data, confirming the good accuracy of the procedure.

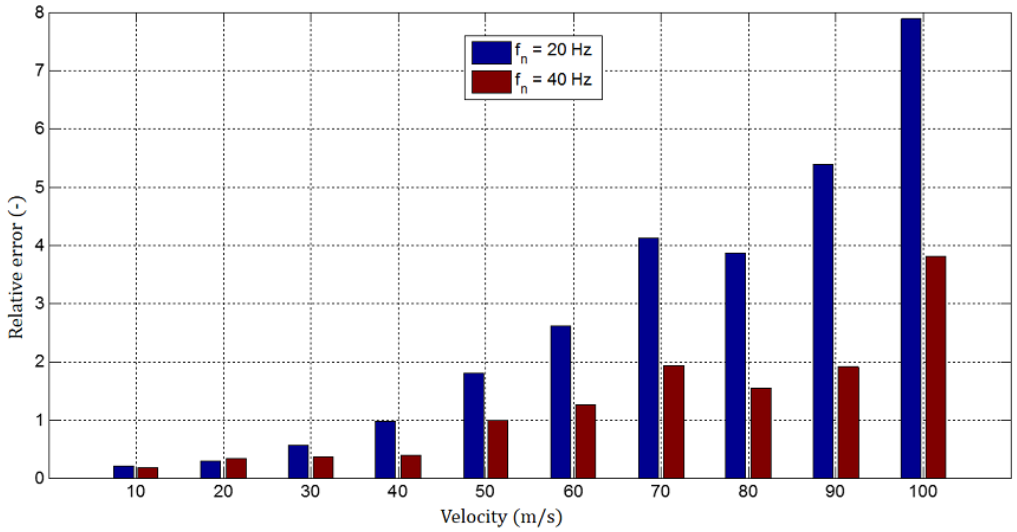

Figure 10. Maximum relative error $e^{sim}_{\max}(V, f_n)$.

Concerning the future developments, other estimation procedures (like weighted least square optimization (WLSO) and nonlinear least square optimization (NLSO)) and other possible physical inputs of the algorithm besides the vertical forces on the sleepers F_{zs} (like generic stresses σ and deformations ε and the longitudinal deformations ε_{xx} as well as a combination of such physical quantities and other measurement layouts) will be considered for estimating the vertical wheel loads $\widehat{N}_{is}$. The authors are currently waiting for receiving from Ansaldo STS extensive experimental data concerning measurement campaigns performed with several vehicles on different railway tracks with different measurement layouts and different measured physical quantities as inputs of the WIM algorithm.

References

[1] S. Iwnicki. *Handbook of Railway Vehicle Dynamics*. Taylor and Francis, 2006.

[2] A. Rindi, L. Pugi, and E. Meli. Weighing in motion of railway vehicles: development and comparison of different identification/measurement techniques. In *European Congress on Computational Methods in Applied Sciences and Engineering (ECCOMAS)*, Vienna, Austria, 10-14 September 2012.

[3] J. Nocedal and S. Wright. *Numerical optimization*. Springer Series in Operation Research, Springer, Berlin, Germany, 1999.

[4] E. Meli, S. Falomi, M. Malvezzi, and A. Rindi. Determination of wheel - rail contact points with semianalytic methods. *Multibody System Dynamics*, 20(4):327–358, 2008.

[5] S. Falomi, M Malvezzi, and E. Meli. Multibody modeling of railway vehicles: innovative algorithms for the detection of wheel-rail contact points. *Wear*, 271(1-2):453–461, 2011.

[6] L. F. Shampine and M. W. Reichelt. The matlab ode suite. *SIAM Journal of Scientific Computation*, 18:1–22, 1997.

[7] C. Kelley. *Iterative methods for linear and nonlinear equations*. SIAM, Philadelphia, PA, USA, 1995.

[8] A.C. Hindmarsh, P.N. Brown, K.E. Grant, D.E. Shumaker, and C.S. Woodward. Sundials: Suite of nonlinear and differential/algebraic equation solvers. *ACM T. Math. Software*, 31:363, 2005.

[9] P.N. Brown, A.C. Hindmarsh, and L.R. Petzold. Using krylov methods in the solution of large-scale differential-algebraic systems. *SIAM J. Sci. Comput*, 15:1467–1488, 1994.

[10] S. Iwnicki. *The Manchester Benchmarks for Rail Vehicle Simulators*. Swets and Zeitlinger, Lisse, Netherland, 1999, 2008.